Cell Switch-Off for Networks Deployed with Variable Spatial Regularity

Faraj Lagum, *Student Member, IEEE,* Quoc-Nam Le-The, Tamer Beitelmal, *Student Member, IEEE,* Sebastian S. Szyszkowicz, *Member, IEEE,* and Halim Yanikomeroglu *Fellow, IEEE*

***Abstract*—Cell switch-off (CSO) is considered to be a promising approach to reduce the energy consumed by cellular networks. In this paper, we set a new CSO research direction that focuses on saving energy and increasing the performance of a network – deployed with variable amounts of spatial regularity – by switching off some cells so as to maximize the spatial regularity of the remaining active cells. We propose three greedy algorithms for tackling this new problem. Among the proposed algorithms, the greedy construction (GC) is the algorithm we choose.**

***Index Terms*—Green communications, energy-efficient, stochastic geometry, point processes, Delaunay triangulation.**

I. Introduction

RECENTLY, cellular networks have witnessed a dramatic growth in demand for data traffic – an approximate 60% rise year-on-year [1] – due to the increase in the number of mobile broadband devices and emerging data-hungry internet applications. This explosion in demand requires an increase in the number of base stations (BSs) in order to alleviate the network's capacity shortage during the peak traffic. As a result, most of these BSs are underutilized during low traffic periods, although they are the significant consumers of cellular network power. Therefore, turning off some BSs while maintaining good service quality, would save a remarkable amount of energy, and hence reduce both the network's operational cost and greenhouse gas emissions [2].

In the current CSO literature, most authors consider the triangular lattice (TL) (i.e., the hexagonal layout): the most regular arrangement for BSs deployment. Recently, a few works such as [3], [4] have modeled the BS locations using the homogeneous Poisson point process (PPP). In general, cellular research focuses either on completely regular (i.e., TL) or on completely random (i.e., PPP) BSs placement. Nevertheless, the actual deployment of BSs most probably lies somewhere in between these two ends of the scale [5]–[7]. Repulsive point processes (RPPs), such as the hard-core processes [6] and perturbed triangular lattices (PTLs) [8], are more realistic tunable models. In particular, the PTLs span the entire range between the TL and the PPP. Therefore, we employ a PTL for modelling the BS locations in this paper. These RPPs have not been used to model the BS locations in the CSO context.

This work is funded by TELUS Corp., an NSERC USRA scholarship, and by the Ministry of Higher Education and Scientific Research (MOHESR), Libya, through the Libyan-North American Scholarship Program

The authors are with the Department of Systems and Computer Engineering, Carleton University, Ottawa, Ontario, Canada. Email: {faraj.lagum, tamer, sz, halim}@sce.carleton.ca, QuocNamLeThe@cmail.carleton.ca.

Motivation: The authors of [9] predicted that "the regularity maximizes the coverage probability." This is confirmed in [6] and [7] for cellular networks by showing that the best signal-to-interference ratio (SIR) distribution is achieved when BSs are placed on the perfect regular TL; the worst is found when the BSs are deployed according to a PPP. The higher the regularity of the BS deployment, the better the coverage probability and SIR distribution. Ideally, the network operators would maintain the coverage requirement or even improve it while saving the energy during low-traffic demand by switching off some BSs. In practice, they may only want to avoid a drastic drop in network coverage. The intuitive approach to attaining the best possible coverage quality is to maximize the regularity of the remaining active BSs. Although there is no explicit research stream focusing on regularity maximization in CSO, this has been done in some previous CSO literature. Some works that use hexagonal layout propose CSO patterns that maintain regularity and provide best possible coverage probability – this is the case in [10], for example. As for a PPP-deployed network, Cho and Choi [3] propose a "*repulsive cell* activation strategy".

Contribution: Our main contribution is that we identify and study a novel CSO problem that has not been previously addressed in the literature. Starting with BSs deployed with a variable amount of spatial regularity, we focus on maximizing the network's performance through maximizing the spatial deployment regularity of the remaining active BSs. As a starting point, we also propose simple and intuitive, yet practical, algorithms to solve this problem. Finally, we apply one of these algorithms to a real set of BSs.

II. CSO as a Regularity Maximization Problem

Given a set of BSs deployed using a repulsive spatial model, we consider switching off some of them in order to save energy during low-traffic periods while maximizing the network performance of the remaining active BSs. An important wireless network performance metric worth maximizing is the coverage probability, which depends on the distribution of the SIR. The network performance can be maximized by maximizing the spatial regularity of the active BSs.

Recently, the regularity of a spatial layout of BSs has been mathematically quantified in a rigorous way using CoV-based scalar metrics [6]. Among these metrics, we choose the CoV of the lengths of Delaunay triangulation edges (C_{D}) to measure the change in regularity resulting from the CSO. As shown in [6], as C_{D} decreases, the spatial regularity increases (i.e.,

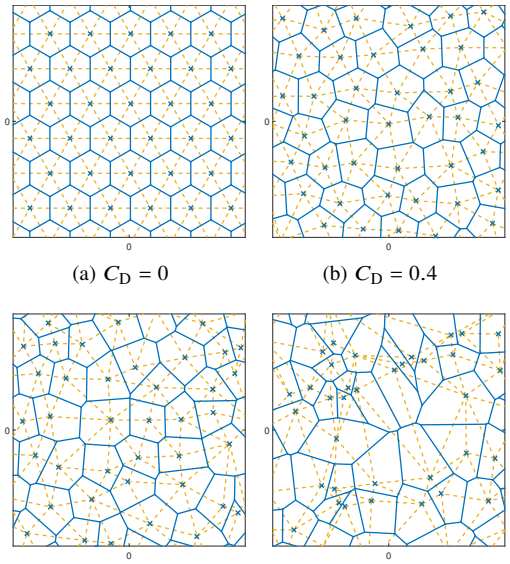

(a) $C_D = 0$ (b) $C_D = 0.4$

(c) $C_D = 0.6$ (d) $C_D = 1$ (PPP)

Fig. 1. Delaunay triangulation (golden dashed lines) and Voronoi tessellation (blue solid lines) of a spatial pattern (blue plus marks) with different amounts of regularity as quantified using C_D.

irregularity decreases). That means that minimizing C_D leads to maximizing the regularity. The metric C_D is presented in detail in the following subsection.

Proposed Regularity Metric: The proposed metric uses the length of the Delaunay triangulation edges[1] to describe the spatial structure of a set of points [6]. The length of these edges is a random quantity. The edges connect each BS to all its *natural neighbors*. For a particular spatial pattern, C_D is the normalized coefficient of variation (CoV), i.e., the ratio of the standard deviation of the edge lengths to their mean:

$$C_D = \frac{1}{k_D} \cdot \frac{\sigma_D}{\mu_D}, \tag{1}$$

where $k_D \cong 0.492$ is a normalization factor such that $C_D = 1$ for the PPP, and μ_D and σ_D are the mean and the standard deviation of the length of Delaunay edges [11], respectively.

Fig. 1 shows realizations of four different network layouts with different amounts of regularity as measured using the C_D metric. The perfect hexagonal layout (Fig. 1a) has $C_D = 0$ (completely regular). At the other end of the RPPs scale, the PPP (Fig. 1d) has $C_D = 1$ (a completely random layout). As the BSs spread out, the regularity increases.

The Problem Statement in Brief: Given a set $\mathcal{A}$ of N BSs, which can be modeled using an RPP, we aim to switch off L BSs and leave the remaining $M = N - L$ BSs active such that their regularity is maximized, thus also maximizing the coverage probability. Our objective is to put the active BSs as far apart from one another as possible. The CSO percentage is $\rho = (L/N) \times 100\%$.

One way to ensure the active BSs are spread out as far as possible is to maximize the nearest neighbor distance for each BS. This is called the p-dispersion problem [12], which is usually formulated as mixed-integer linear programming and has been known to be NP-hard [12].

[1]Note that in order to eliminate the edge effect, Delaunay edges between points on the border of the considered region should not be taken into consideration for calculating the C_D.

III. Proposed Algorithms for Cell Switch-Off

Due to the difficulty of solving this problem optimally, we propose three greedy heuristic algorithms to tackle it.

Greedy Construction (GC): The solution set of the GC is initialized by selecting the two furthest points. Then, at each iteration, a new point, the one furthest apart from all points in this solution set, is added until the targeted number of active points M is accumulated in the solution set [12]. The complexity of the GC in terms of distance computation is $O(N^2)$ for finding the two furthest points and $O(M^2N)$ for the rest of the algorithm.

Greedy Deletion (GD): The GD is initialized by identifying the two closest BSs in the current solution set and switching off the one that has the smallest distance to its second-nearest neighbor. This is repeated until the specified number of BSs is turned off [12]. The complexity of the GD in is $O(N^3)$.

Semi-Greedy Deletion (SG): This is very similar to the GD algorithm. The only difference is that it employs random selection for removal between the two closest points [12].

Random Switch-Off (RS): BSs are randomly switched off without any rules apart from the number of BSs required to be off [4]. This represents the lower bound.

Moreover, separate *PPP-deployed* and *TL-deployed* networks – that have the same density as the remaining active BSs of the partially switched-off network – are used as a loose lower bound and a non-achievable upper bound, respectively.

IV. System Model

BS Deployment: We consider a network layout modeled using Perturbed Triangular Lattice (PTL) [7], [8], an RPP with variable regularity. The advantage of the PTL model is that it covers the whole range between the TL and the PPP [8], unlike many RPPs [6]. Generating the PTL starts with generating TL, and then independently perturbing each point (BS location) by a random independent vector. We consider uniform displacement on a disk which leads to uniform PTL. The radius R of the disk controls the amount of regularity. It is normalized by the inter-site distance η of the TL as $\tilde{R} = R\eta^{-1}$. The metric C_D is then a function of $\tilde{R}$. The density of the TL and also the PLT is $\lambda = \frac{2}{\sqrt{3}}\eta^{-2}$. Details are presented in [8].

Downlink Channel Model: Independent of the network deployment, the users are modeled as a PPP. Each user is tagged to the strongest BS. users have best effort service with equal resource allocation. They receive Rayleigh faded signals with mean 1. All the BSs serve with full buffer and transmit at the same fixed power level and have the same operating frequency. They have one sector and single antenna.

LTE urban macro (UMa) scenario. Channel parameters and all other specifications follow the UMa scenario presented in [13]. We assume the proportional fair scheduling scheme.

Simple scenario. We only consider this simple scenario for calculating SIR gain to make some of the results comparable with [14]. It has simple path loss model with a path loss exponent of 4 and no shadowing. The thermal noise is ignored.

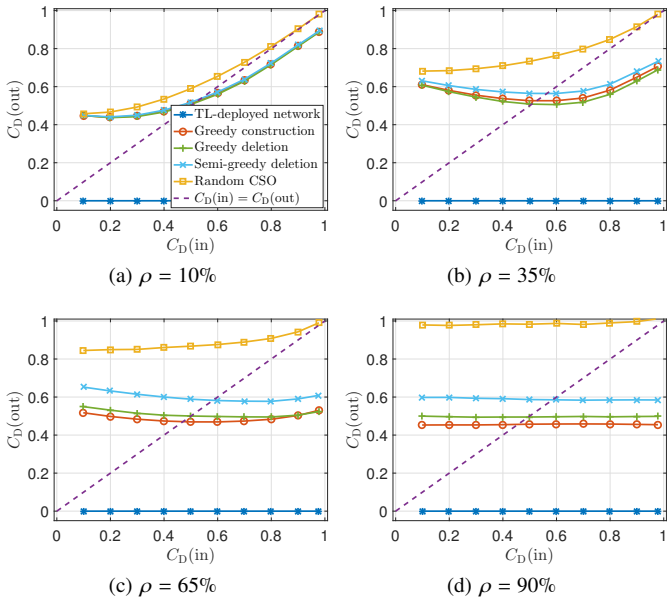

(a) ρ = 10% (b) ρ = 35% (c) ρ = 65% (d) ρ = 90%

Fig. 2. Network deployment regularity before (C_D(in)) and after (C_D(out)) applying the CSO algorithms at different CSO percentages ρ.

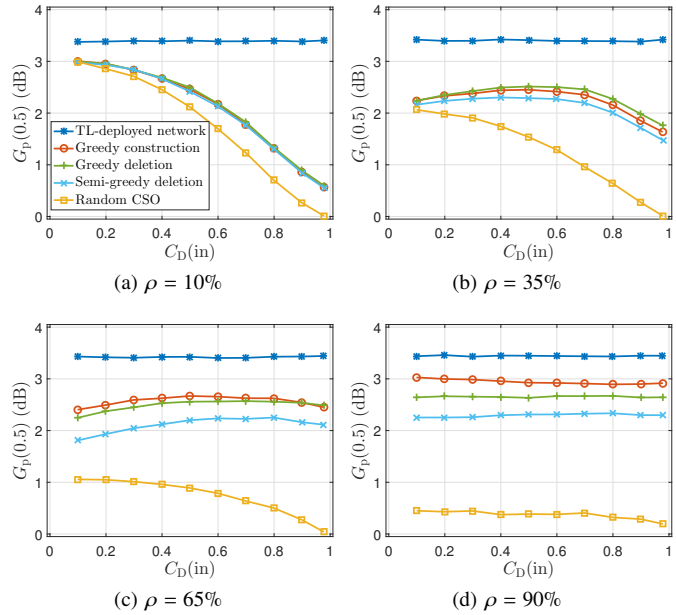

(a) ρ = 10% (b) ρ = 35% (c) ρ = 65% (d) ρ = 90%

Fig. 3. The SIR gain $G_p(0.5)$ as a function of the network deployment regularity before the CSO (C_D(in)) at different CSO percentages ρ.

V. Results

We consider a network with 665 BSs deployed over an area of 12 km × 12 km. 10 users per BS are distributed over the whole area, but we only consider users within the central area of 7.2 km × 7.2 km in order to eliminate the edge effects. We sweep the BS regularity from TL ($C_D = 0$) to PPP (asymptotically, $C_D \to 1$) using the tunable PTL. We apply the CSO algorithms presented in Section III on these BS deployments. With 5% steps, we switch off up to 90% of the BSs. The saved energy is proportional to the number of turned-off BSs [10]. For brevity, only specific CSO percentage ρ values are reported in Figs. 2–6.

Fig. 2 shows the change in the network regularity before (C_D(in)) and after (C_D(out)) applying the CSO algorithms. The lower the C_D value, the higher the regularity of BSs. For BSs deployed with very high regularity, the proposed CSO algorithms deteriorate their regularity. However, this may still be close to the best achievable regularity if some of the BSs are switched off. The greedy algorithms improve the spatial regularity when the BSs are deployed with low regularity ($C_D \gtrsim 0.5$). The line C_D(out) = C_D(in) separates the graphs in Fig. 2 into two regions: above the line, where the regularity is deteriorated, and below, where the regularity is improved.

SIR gain. Taking a PPP-deployed network as a reference, we use the horizontal gap (SIR gain) between the SIR distributions of the PPP- and the PTL-deployed networks as the performance metric; specifically, the SIR gain at target probability 50 percent: $G_p(0.5)$ [7], [14]. Fig. 3 shows the comparison between different CSO algorithms at different ρ values in terms of the SIR gain for BSs deployed with variable amounts of regularity.

Fig. 2 shows that as the degree of freedom increases for high ρ values, the algorithms significantly enhance the regularity (e.g., reducing C_D to around 0.4 for GC). The SIR gain is hence improved in Fig. 3. Being completely regular, TL-deployed network has an SIR gain of 3.4 dB, the highest SIR gain compared to a PPP-deployed with Simple scenario assumptions in Section IV. This 3.4 dB is consistent with the literature [14]. In terms of regularity and SIR gain, the SG algorithm does not perform as well. While GD algorithm performs better for low CSO percentage ($\rho < 55\%$), the GC dominates for higher ρ values. An interesting observation is that even when GD performs better, GC still performs comparably well, within a 0.1 dB SIR difference. Thus, if an operator must select only one algorithm for the entire switch-off scale, we recommend GC.

Note that GD and SG usually make bad decisions when they are applied on the TL, since all points are equally spaced. Thus, we exclude applying the CSO algorithms on the idealized TL deployment from this work.

Network capacity. We define the network capacity as the sum of rates of all users in the system in bits/s/Hz. The normalized[2] capacity as a function CSO percentage for different CSO algorithms is shown in Fig. 4. The number of the switched-off BSs is a function of the decrease in the network's data traffic. For a network deployed according to a PPP (see Fig. 4b), if the network traffic is dropped by 20%, unlike the RS where it is possible to switch off ≈ 20% of the BSs, the operator could switch off up to ≈ 37% of BSs using the greedy algorithms when they consider maximizing the regularity of the remaining active cells.

Rate coverage. Defining the rate coverage as the probability that a randomly located user achieves a rate greater than the rate threshold $\mathcal{R}_{th}$, the coverage probability of the rate $\mathcal{R}_{th}$ = 512 kbps for two BS deployments as a function of the CSO values with applying different CSO algorithms is shown in

[2]We normalize the capacity of each deployment by its full capacity before the switch-off.

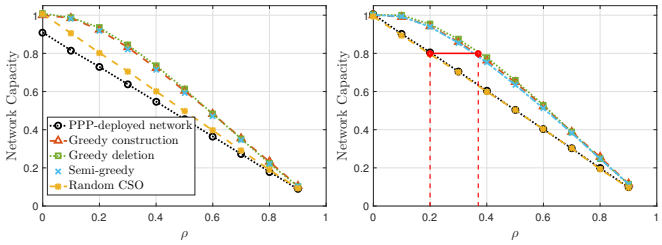

(a) $C_{\mathrm{D}}(\mathrm{in}) = 0.8$ (b) $C_{\mathrm{D}}(\mathrm{in}) = 1$ (PPP)

Fig. 4. Normalized network capacity for LTE UMa scenario as a function of the CSO percentages ρ for two different network deployment in terms of regularity. The regularity maximization gain is annotated by thick red line (b).

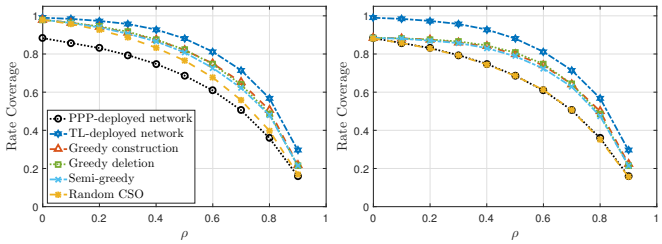

(a) $C_{\mathrm{D}}(\mathrm{in}) = 0.4$ (b) $C_{\mathrm{D}}(\mathrm{in}) = 1$ (PPP)

Fig. 5. Rate coverage for LTE UMa scenario as a function of the CSO percentages ρ for two different network deployment in terms of regularity.

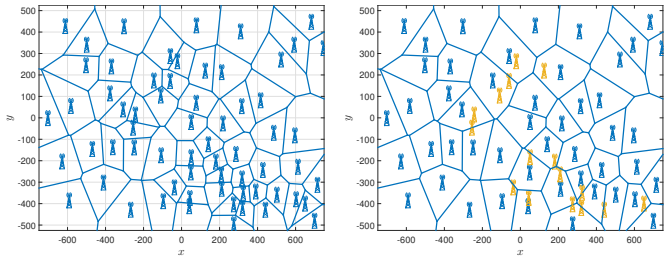

(a) Real data, $C_{\mathrm{D}} = 0.806$ (b) $\rho = 25\%$, $C_{\mathrm{D}} = 0.61$

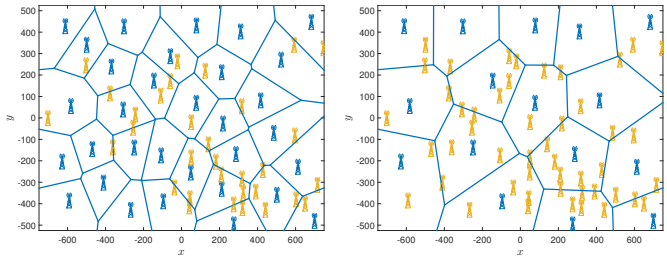

(c) $\rho = 50\%$, $C_{\mathrm{D}} = 0.46$ (d) $\rho = 75\%$, $C_{\mathrm{D}} = 0.35$

Fig. 6. Applying the greedy deletion algorithm on real BS locations at different CSO percentages ρ. Blue and golden towers represent the active and inactive BSs, respectively. The BSs (GSM band 900 MHz) belong to the Vodafone operator. The region is $1500\,\mathrm{m} \times 1050\,\mathrm{m}$, in London, UK, centered at (51.5136°N, 0.1342°W). This data is similar to that used in [7, Fig. 1].

Fig. 5. With regularity maximization algorithms, users achieve higher rates compared to RS.

Real BS locations. As an example, we apply the GD on a real deployment of BSs, taken from Ofcom[3] and shown in Fig. 6. As depicted in Fig. 6, as more BSs are switched off, the previously turned-off BSs are never turned back on.

The advantage of GC and GD is that the current solution is a subset of the previous solution if ρ is increased and a superset if ρ is decreased. That is, the CSO has the same pattern: the first switched-off BS is the last to be turned on when the ρ changes. This is a very practical feature for cellular network operators since it reduces the on-off/off-on transitions. The disadvantage is that the accuracy of the solution may decrease for GC if the targeted number of the BSs for switching-off is low and for GD if the targeted number is high.

VI. Conclusion

This work expands the CSO literature by modelling BSs using RPPs. We shed light on a new CSO problem that relates the network's performance improvement to the maximization of the regularity of the active cells. With regularity maximization CSO, extra BSs could be turned off while maintaining the same quality-of-service compared to RS. The regularity maximization gain is significant for highly irregular BS deployments. Testing other heuristics and deriving mathematical expression for coverage probability as a function of CSO percentage are reserved for future work.

[3]Independent regulator and competition authority for the UK communications industries. Ofcom website: http://www.sitefinder.ofcom.org.uk/

References

[1] Ericsson, "Ericsson mobility report," Tech. Rep., June 2016.

[2] Ł. Budzisz *et al.*, "Dynamic resource provisioning for energy efficiency in wireless access networks: A survey and an outlook," *IEEE Commun. Surveys Tuts.*, vol. 16, no. 4, pp. 2259–2285, 4th quarter 2014.

[3] S. Cho and W. Choi, "Energy-efficient repulsive cell activation for heterogeneous cellular networks," *IEEE J. Sel. Areas Commun.*, vol. 31, no. 5, pp. 870–882, May 2013.

[4] S. S. Kumar and A. Kumar, "Energy efficient rate coverage with base station switching and load sharing in cellular networks," in *IEEE Int. Conf. Commun. Syst. and Netw. (COMSNETS)*, Jan. 2016, pp. 1–6.

[5] J. Andrews, "Seven ways that HetNets are a cellular paradigm shift," *IEEE Commun. Mag.*, vol. 51, no. 3, pp. 136–144, Mar. 2013.

[6] F. Lagum, S. Szyszkowicz, and H. Yanikomeroglu, "CoV-based metrics for quantifying the regularity of hard-core point processes for modeling base station locations," *IEEE Wireless Commun. Lett.*, vol. 5, no. 3, pp. 276–279, June 2016.

[7] A. Guo and M. Haenggi, "Spatial stochastic models and metrics for the structure of base stations in cellular networks," *IEEE Trans. Wireless Commun.*, vol. 12, no. 11, pp. 5800–5812, Nov. 2013.

[8] F. Lagum, S. S. Szyszkowicz, and H. Yanikomeroglu, "Quantifying the regularity of perturbed triangular lattices using CoV-based metrics for modeling the locations of base stations in HetNets," in *IEEE Veh. Technol. Conf. (VTC2016-Fall)*, Sept. 2016, pp. 1–5.

[9] R. Ganti and M. Haenggi, "Regularity in sensor networks," in *IEEE Int. Zurich Seminar Commun.*, Feb. 2006, pp. 186–189.

[10] A. Kumar and C. Rosenberg, "Energy and throughput trade-offs in cellular networks using base station switching," *IEEE Trans. Mobile Comput.*, vol. 15, no. 2, pp. 364–376, Feb. 2016.

[11] M. Mirahsan, R. Schoenen, and H. Yanikomeroglu, "HetHetNets: Heterogeneous traffic distribution in heterogeneous wireless cellular networks," *IEEE J. Sel. Areas Commun.*, vol. 33, no. 10, pp. 2252–2265, Oct. 2015.

[12] E. Erkut, Y. Ülküsal, and O. Yenicerioğlu, "A comparison of p-dispersion heuristics," *Computers & Operations Research*, vol. 21, no. 10, pp. 1103–1113, Dec. 1994.

[13] M. Series, "Guidelines for evaluation of radio interface technologies for IMT-Advanced," 2009.

[14] M. Haenggi, "The mean interference-to-signal ratio and its key role in cellular and amorphous networks," *IEEE Wireless Commun. Lett.*, vol. 3, no. 6, pp. 597–600, Sept. 2014.